

# Nanoscale

Accepted Manuscript



This is an *Accepted Manuscript*, which has been through the Royal Society of Chemistry peer review process and has been accepted for publication.

*Accepted Manuscripts* are published online shortly after acceptance, before technical editing, formatting and proof reading. Using this free service, authors can make their results available to the community, in citable form, before we publish the edited article. We will replace this *Accepted Manuscript* with the edited and formatted *Advance Article* as soon as it is available.

You can find more information about *Accepted Manuscripts* in the [Information for Authors](#).

Please note that technical editing may introduce minor changes to the text and/or graphics, which may alter content. The journal's standard [Terms & Conditions](#) and the [Ethical guidelines](#) still apply. In no event shall the Royal Society of Chemistry be held responsible for any errors or omissions in this *Accepted Manuscript* or any consequences arising from the use of any information it contains.

## ARTICLE

# Advanced Use of High-Performance Liquid Chromatography for Synthesis of Controlled Metal Clusters

Cite this: DOI: 10.1039/x0xx00000x

Yoshiki Niihori,<sup>a</sup> Miku Matsuzaki,<sup>a</sup> Chihiro Uchida,<sup>a</sup> and Yuichi Negishi<sup>\*. a,b</sup>

Received 00th January 2012,

Accepted 00th January 2012

DOI: 10.1039/x0xx00000x

[www.rsc.org/](http://www.rsc.org/)

Because the synthesis of metal clusters with multiple ligand types results in a distribution of ligands, high-resolution separation of each unique cluster from the mixture is required for precise control of the ligand composition. Reverse-phase high-performance liquid chromatography combined with appropriate transitioning of the mobile phase composition is an extremely effective means of separating ligand combinations when working with metal clusters protected by two different types of thiolates. We report herein advanced use of this method. The studies involving  $\text{Au}_{24}\text{Pd}(\text{SR}_1)_{18-x}(\text{SR}_2)_x$  and  $\text{Au}_{24}\text{Pd}(\text{SR}_1)_{18-x}(\text{SeR}_2)_x$  ( $\text{SR}_1, \text{SR}_2 = \text{thiolate}, \text{SeR}_2 = \text{selenolate}$ ) revealed the followings. (1) In general, an increase in the difference between the polarities of the functional groups incorporated in the two types of ligands improves the separation resolution. A suitable ligand combination for separation can be predicted from the retention times of  $\text{Au}_{24}\text{Pd}(\text{SR}_1)_{18}$  and  $\text{Au}_{24}\text{Pd}(\text{SR}_2)_{18}$ , which cause the terminal peaks in a series of peaks. (2) The use of a step-gradient program during the mobile phase substitution results in improved resolution compared to that achievable with the linear gradients applied in prior work. (3) This technique is also useful for the evaluation of the chemical compositions of metal clusters protected by two different types of ligands with similar molecular weights. These findings will provide clear design guidelines for the functionalization of metal clusters via control of the ligand composition, and will also improve our understanding of the high-resolution isolation of metal clusters.

## Introduction

Advances in nanotechnology have encouraged the creation of nanomaterials that are both stable and highly functionalized. Thiolate-protected gold clusters ( $\text{Au}_n(\text{SR})_m$ )<sup>1–13</sup> less than 2 nm in size have attracted a great deal of attention as new functionalized nanomaterials since they are highly stable compared to other metal clusters and also exhibit size-specific and size-dependent physical and chemical properties, including photoluminescence,<sup>3,4,7,14</sup> redox behavior<sup>3,7</sup> and catalytic activity,<sup>15</sup> that are not observed in the case of bulk gold.

These  $\text{Au}_n(\text{SR})_m$  clusters are generally prepared via the reduction of gold ions in solution in the presence of thiols.<sup>1,16</sup> However, this method tends to yield a mixture of  $\text{Au}_n(\text{SR})_m$  clusters with various core sizes.<sup>17,18</sup> High-resolution isolation of clusters of each size from the mixture is therefore important so as to obtain  $\text{Au}_n(\text{SR})_m$  clusters with well controlled physical and chemical properties. Previous research has demonstrated that polyacrylamide gel electrophoresis<sup>4,17,18</sup> and high performance liquid chromatography (HPLC)<sup>19,20</sup> are extremely effective means of separating hydrophilic thiolate-protected  $\text{Au}_n(\text{SR})_m$  clusters, and that both solvent extraction<sup>4,21,22</sup> and HPLC<sup>23,24</sup> are highly efficient techniques for the separation of hydrophobic thiolate-protected  $\text{Au}_n(\text{SR})_m$  clusters. The characterization of clusters isolated in this manner, using mass

spectrometry,<sup>4,17,18,22,25–27</sup> enables the precise synthesis of numerous  $\text{Au}_n(\text{SR})_m$  clusters ( $n \leq 333$ ; ref. 28) with accuracy at the atomic level.

In addition to their core sizes, the physical and chemical properties of  $\text{Au}_n(\text{SR})_m$  clusters vary depending on the particular ligands that cover the clusters. For example, the solubilities and photoluminescence quantum yields<sup>29</sup> of thiolate-based clusters vary depending on the thiolate functional group. Moreover, the use of a thiolate with a specific functionality as the ligand endows  $\text{Au}_n(\text{SR})_m$  clusters with functions such as molecular recognition or catalytic abilities.<sup>30</sup> In addition, the use of selenolate ( $\text{SeR}$ )<sup>16,31,32</sup> as the ligand changes the charge transfer at the metal core interface,<sup>32–35</sup> resulting in clusters that are more stable than the  $\text{Au}_n(\text{SR})_m$  clusters.<sup>33,35</sup> Control of the ligand composition is therefore an effective way of controlling the cluster functionality. Thus, if we can obtain the desired ligand composition, the functions of the resulting clusters can be finely tuned and arrangement of the clusters in certain patterns can also be achieved. However, except in a limited number of cases,<sup>36</sup> the synthesis of clusters with multiple types of ligands results in a distribution of ligand chemical compositions and so precise control over the ligand composition requires high-resolution separation of each chemical composition from the mixture.<sup>37–40</sup>

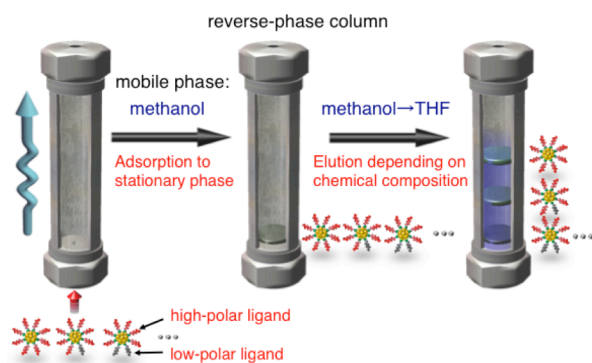


**Chart 1.** Schematic diagram of the high-resolution separation of metal clusters containing two different types of ligand by HPLC using a reverse phase column with a mobile phase gradient.<sup>42</sup>

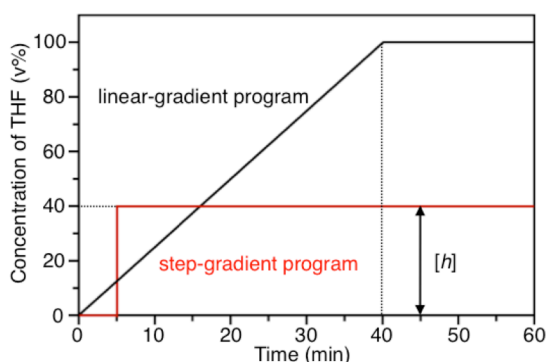


**Chart 2.** Mobile phase gradients used in this work: (black) linear and (red) step. In the step gradient, the step height [h] indicates the volume percent of THF after transition of the mobile phase. Methanol was used as the initial adsorption solvent for these experiments.

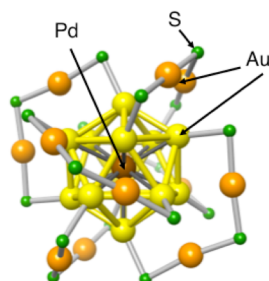


**Chart 3.** Structural representation of  $\text{Au}_{24}\text{Pd}(\text{SR})_{18}$ .<sup>45,46</sup> The R moieties have been omitted for clarity.

Several studies have demonstrated that HPLC is also a useful method for such separations.<sup>41–43</sup> Recently, using a method that combines reverse phase HPLC with mobile phase substitution based on a linear gradient, we achieved the high-resolution separation of  $\text{Au}_{24}\text{Pd}(\text{SC}_{12}\text{H}_{25})_{18-x}(\text{SCH}_2\text{Ph}^t\text{Bu})_x$  ( $x = 0–18$ ,  $\text{SCH}_2\text{Ph}^t\text{Bu} = 4$ -*tert*-butylphenylmethanethiolate), a cluster protected by two different types of thiolate ligands.<sup>42</sup> In this method, a mixture of clusters is initially adsorbed onto the stationary phase, after which the clusters are sequentially eluted via continuous transformation of the mobile phase to a solvent capable of dissolving the clusters. This is accomplished by

**Table 1.** Ligand combinations applied in this study

Entry	SR <sub>1</sub>	Mw <sub>av</sub> <sup>a</sup>	SR <sub>2</sub> /SeR <sub>2</sub>	Mw <sub>av</sub> <sup>a</sup>
1	SC <sub>12</sub> H <sub>25</sub>	201.39	SC <sub>8</sub> H <sub>17</sub>	145.29
2	SC <sub>12</sub> H <sub>25</sub>	201.39	SC <sub>6</sub> H <sub>13</sub>	117.23
3	SC <sub>12</sub> H <sub>25</sub>	201.39	SC <sub>4</sub> H <sub>9</sub>	89.18
4	SC <sub>12</sub> H <sub>25</sub>	201.39	SCH <sub>2</sub> Ph <sup>t</sup> Bu <sup>b</sup>	179.30
5	SC <sub>12</sub> H <sub>25</sub>	201.39	SCH <sub>2</sub> PhBr <sup>c</sup>	202.09
6	SC <sub>12</sub> H <sub>25</sub>	201.39	SC <sub>2</sub> H <sub>4</sub> Ph	137.22
7	SC <sub>2</sub> H <sub>4</sub> Ph	137.22	SC <sub>14</sub> H <sub>29</sub>	229.45
8	SC <sub>2</sub> H <sub>4</sub> Ph	137.22	SC <sub>10</sub> H <sub>21</sub>	173.34
9	SC <sub>2</sub> H <sub>4</sub> Ph	137.22	SC <sub>6</sub> H <sub>13</sub>	117.23
10	SC <sub>2</sub> H <sub>4</sub> Ph	137.22	SeC <sub>12</sub> H <sub>25</sub>	248.29
11	SC <sub>12</sub> H <sub>25</sub>	201.39	SeC <sub>12</sub> H <sub>25</sub>	248.29

<sup>a</sup>Average molecular weight calculated using the Bunshiro software package.

<sup>b</sup>4-*tert*-Butylphenylmethanethiolate (Chart S1a). Note that this molecule was abbreviated as SBB in a previous paper.<sup>42</sup> <sup>c</sup>4-Bromophenylmethanethiol (Chart S1b).

applying a linear gradient which gradually substitutes the mobile phase composition (Charts 1 and 2). Using this approach, clusters corresponding to each unique ligand combination,  $\text{Au}_{24}\text{Pd}(\text{SC}_{12}\text{H}_{25})_{18-x}(\text{SCH}_2\text{Ph}^t\text{Bu})_x$  ( $x = 0–18$ ), were successfully isolated with high resolution.<sup>42</sup>

Herein we report advanced use of this method. The studies of the  $\text{Au}_{24}\text{Pd}(\text{SR}_1)_{18-x}(\text{SR}_2)_x$  and  $\text{Au}_{24}\text{Pd}(\text{SR}_1)_{18-x}(\text{SeR}_2)_x$  (SR<sub>1</sub>, SR<sub>2</sub> = thiolate, SeR<sub>2</sub> = selenolate) series of clusters have revealed: (1) the ligand combinations suited to high-resolution separation, (2) the gradient program that achieves higher resolution than was achievable with our previously reported gradient program and (3) the advantages of the method with regard to the characterization of clusters. Our previous study indicated that this technique is also applicable to various thiolate-protected metal clusters which have metal cores other than  $\text{Au}_{24}\text{Pd}$ .<sup>42</sup> The findings obtained in this work can thus also be expected to hold true for other thiolate-protected metal clusters. The results reported herein should serve to deepen our understanding of the high-resolution isolation of metal clusters, and will provide clear design guidelines for the functionalization of metal clusters via control of the ligand composition.

## Results and Discussion

Our previous studies have shown that the palladium-doped cluster  $\text{Au}_{24}\text{Pd}(\text{SR})_{18}$  (Chart 3; refs. 44–46) is highly stable in solution<sup>45</sup> and that  $\text{Au}_{24}\text{Pd}(\text{SR}_1)_{18-x}(\text{SR}_2)_x$  clusters, which are protected by two different types of thiolate ligands (SR<sub>1</sub> and SR<sub>2</sub>), can be separated with higher resolution than either  $\text{Au}_{25}$  or  $\text{Au}_{38}$  clusters protected with the same ligands ( $\text{Au}_{25}(\text{SR}_1)_{18-x}(\text{SR}_2)_x$  or  $\text{Au}_{38}(\text{SR}_1)_{24-x}(\text{SR}_2)_x$ ).<sup>42</sup> We therefore employed  $\text{Au}_{24}\text{Pd}$  clusters during the present study. These clusters, protected by two different types of ligands, were synthesized by first synthesizing  $\text{Au}_{24}\text{Pd}$  clusters with one type of thiolate (SR<sub>1</sub>) and then reacting these clusters with the second ligand (R<sub>2</sub>SH or (R<sub>2</sub>Se)<sub>2</sub>, where SeR<sub>2</sub> = selenolate) in dichloromethane via a ligand-exchange reaction (see Experiments for details).<sup>47–51</sup> The ligand combinations (SR<sub>1</sub> and SR<sub>2</sub>/SeR<sub>2</sub>) applied in this study are summarized in Table 1. The ligand distributions in the resulting  $\text{Au}_{24}\text{Pd}(\text{SR}_1)_{18-x}(\text{SR}_2)_x$  (Figures S1–S9) and  $\text{Au}_{24}\text{Pd}(\text{SR}_1)_{18-x}(\text{SeR}_2)_x$  (Figures S10 and

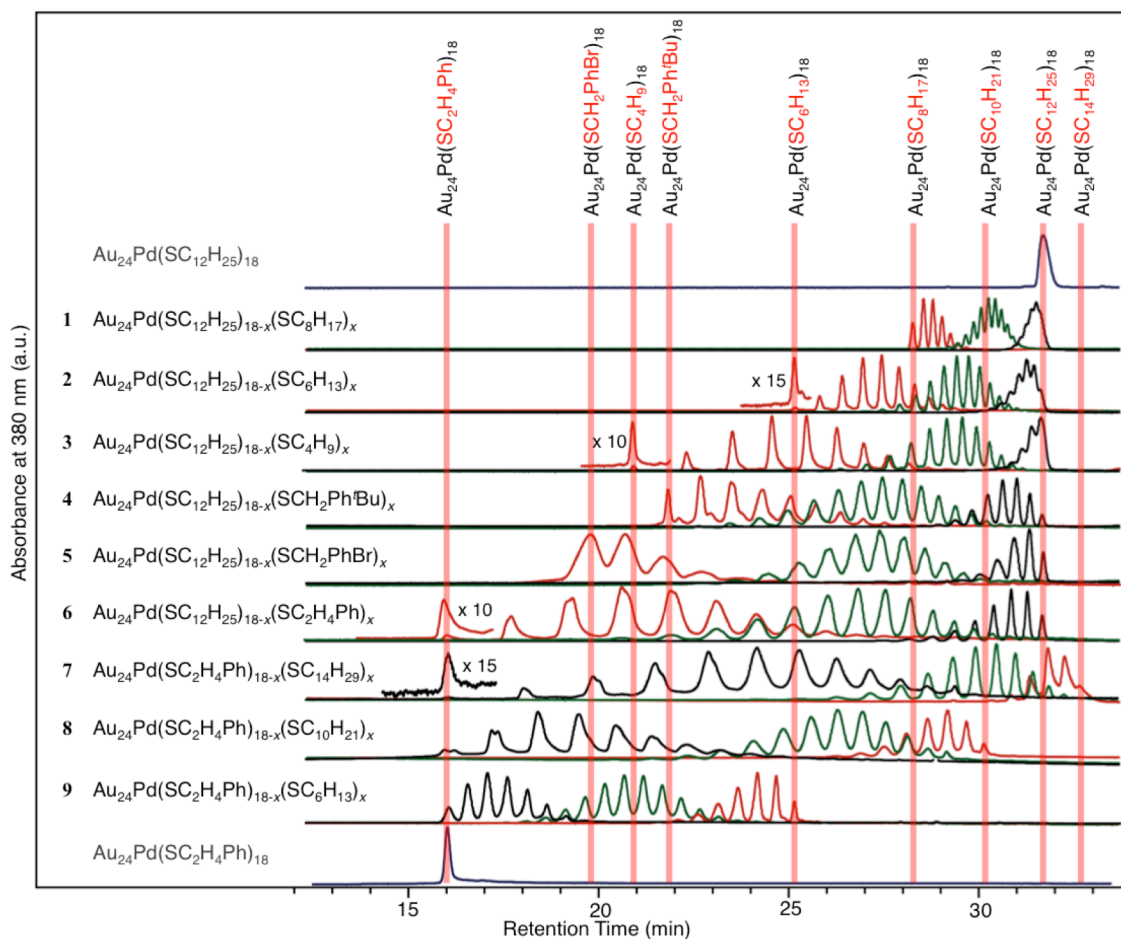


**Figure 1.** Chromatograms obtained for  $\text{Au}_{24}\text{Pd}(\text{SR}_1)_{18-x}(\text{SR}_2)_x$  ( $x = 0-18$ ) clusters with the ligand combinations shown in Table 1, together with those for  $\text{Au}_{24}\text{Pd}(\text{SC}_{12}\text{H}_{25})_{18}$  and  $\text{Au}_{24}\text{Pd}(\text{SC}_2\text{H}_4\text{Ph})_{18}$  for comparison purposes. MALDI mass spectra of each  $\text{Au}_{24}\text{Pd}(\text{SR}_1)_{18-x}(\text{SR}_2)_x$  are provided in Figures S1–S9. In these experiments, the linear-gradient program in Chart 2 was used for replacement of the solvent. In chromatograms (Figure 1) and MALDI mass spectra (Figures S1–S9) for each entry, the same color indicates the same sample; values of  $x$  are small for black line, medium for green line, and large for red line (Figures S1–S9). Red vertical lines indicate the retention times estimated for  $\text{Au}_{24}\text{Pd}$  clusters protected with one type of ligand, i.e.,  $\text{Au}_{24}\text{Pd}(\text{SR}_1)_{18}$  and  $\text{Au}_{24}\text{Pd}(\text{SR}_2)_{18}$ .

S11) clusters were found to vary depending on the reaction conditions.<sup>42,51</sup> The  $\text{Au}_{24}\text{Pd}$  clusters thus obtained with each unique combination of ligands were separated using a method that combines reverse phase HPLC with mobile phase substitution (Chart 2).

**Suitable Ligand Combinations.** During HPLC separations, the mobile phase composition was initially substituted by applying a linear gradient shown in Chart 2. Figure 1 presents the chromatograms obtained for the  $\text{Au}_{24}\text{Pd}(\text{SR}_1)_{18-x}(\text{SR}_2)_x$  series of clusters, corresponding to entries 1–9 in Table 1, along with the chromatograms of  $\text{Au}_{24}\text{Pd}(\text{SC}_{12}\text{H}_{25})_{18}$  and  $\text{Au}_{24}\text{Pd}(\text{SC}_2\text{H}_4\text{Ph})_{18}$  for comparison purposes (see also Figure S12). Well resolved and relatively intense peak structures were observed in all the chromatograms and the distribution of peaks in each individual chromatogram is similar to the peak distribution observed in the matrix-assisted laser desorption–ionization (MALDI) mass spectra of the corresponding clusters (Figures S1–S9). These results indicate that this method was capable of separating all the  $\text{Au}_{24}\text{Pd}(\text{SR}_1)_{18-x}(\text{SR}_2)_x$  clusters (entries 1–9) with high resolution. In the case of the clusters corresponding to entries 1–6, the latest peaks appear at approximately the same retention time in all six chromatograms. The retention time region in which these peaks appear is

approximately the same as the retention time of  $\text{Au}_{24}\text{Pd}(\text{SC}_{12}\text{H}_{25})_{18}$  (Figure 1) and thus these peaks are attributable to the presence of  $\text{Au}_{24}\text{Pd}(\text{SC}_{12}\text{H}_{25})_{18}$  clusters. Similarly, the first peaks in the chromatograms of the entries 6–9 clusters all appear at approximately the same retention time, and these peaks are attributed to  $\text{Au}_{24}\text{Pd}(\text{SC}_2\text{H}_4\text{Ph})_{18}$  (Figure 1). Thus, the peaks on the peripheries of the chromatograms obtained from the  $\text{Au}_{24}\text{Pd}(\text{SR}_1)_{18-x}(\text{SR}_2)_x$  clusters originate from  $\text{Au}_{24}\text{Pd}(\text{SR}_1)_{18}$  and  $\text{Au}_{24}\text{Pd}(\text{SR}_2)_{18}$ . The retention times of the  $\text{Au}_{24}\text{Pd}(\text{SR})_{18}$  clusters increased in the functional group order:  $\text{C}_2\text{H}_4\text{Ph} < \text{CH}_2\text{PhBr} < \text{C}_4\text{H}_9 < \text{CH}_2\text{Ph}^t\text{Bu} < \text{C}_6\text{H}_{13} < \text{C}_8\text{H}_{17} < \text{C}_{10}\text{H}_{21} < \text{C}_{12}\text{H}_{25} < \text{C}_{14}\text{H}_{29}$  (Figure 1). Under the conditions used in our experiments, the clusters with higher polarities are the first to be eluted into the mobile phase. These results demonstrate that the polarity of the functional group decreases in this order. In general, the resolution of each chromatogram was observed to increase with increasing differences in the polarities of the functional groups of the two types of thiolate ligands (Figure 1). These results clearly show that, in order to obtain high-resolution separation of the  $\text{Au}_{24}\text{Pd}(\text{SR}_1)_{18-x}(\text{SR}_2)_x$  clusters, it is vital to increase the difference between the polarities of the functional groups in the two different ligands. These data also demonstrate that a

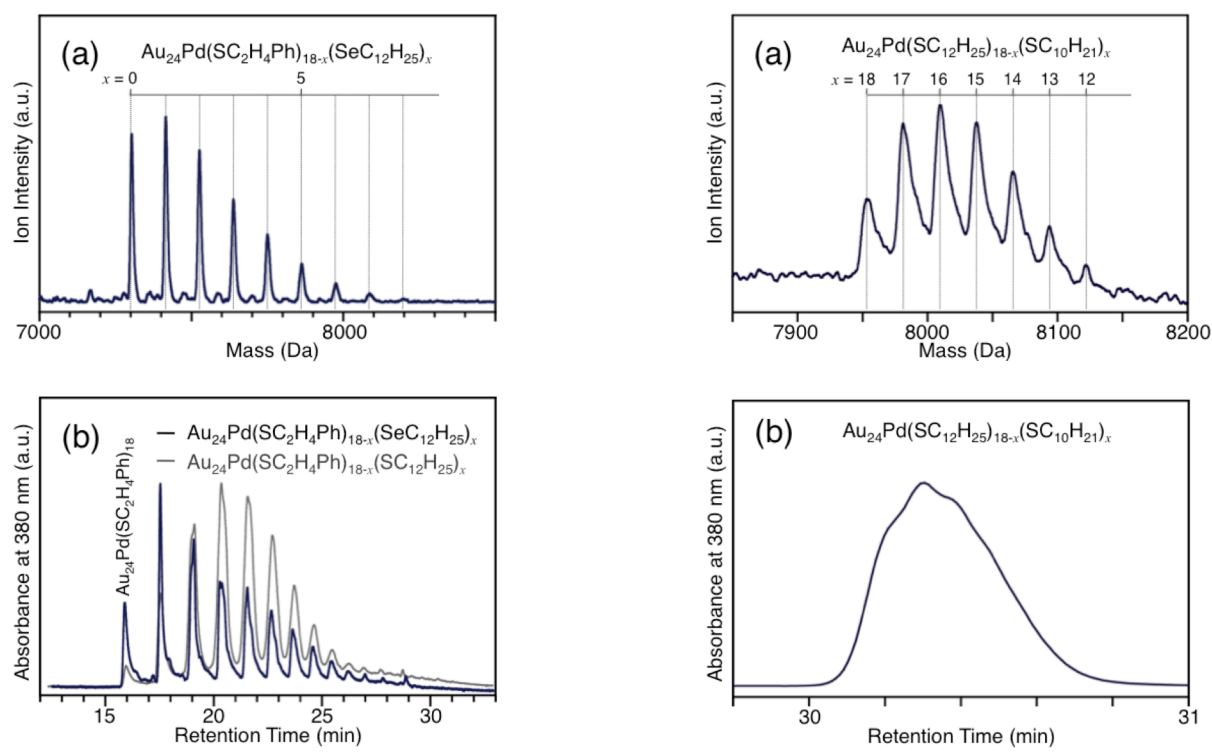


**Figure 2.** (a) Negative-ion MALDI mass spectrum and (b) chromatograms of  $\text{Au}_{24}\text{Pd}(\text{SC}_2\text{H}_4\text{Ph})_{18-x}(\text{SeC}_{12}\text{H}_{25})_x$  ( $x = 0-8$ ) and  $\text{Au}_{24}\text{Pd}(\text{SC}_2\text{H}_4\text{Ph})_{18-x}(\text{SC}_{12}\text{H}_{25})_x$  ( $x = 0-8$ ) for comparison. In (b), the leftmost peak is assigned to  $\text{Au}_{24}\text{Pd}(\text{SC}_2\text{H}_4\text{Ph})_{18}$  (Figure 1).

suitable ligand combination for the separation can be predicted from the retention times of  $\text{Au}_{24}\text{Pd}(\text{SR}_1)_{18}$  and  $\text{Au}_{24}\text{Pd}(\text{SR}_2)_{18}$ , which cause the terminal peaks of a series of peaks.

We found that equivalent high-resolution separation is also achievable in the case of  $\text{Au}_{24}\text{Pd}(\text{SR}_1)_{18-x}(\text{SeR}_2)_x$  clusters, in which SR and SeR are used as the two different types of ligands, when a suitable combination of functional groups is employed. Figures 2a and 2b show the MALDI mass spectrum and chromatogram of  $\text{Au}_{24}\text{Pd}(\text{SC}_2\text{H}_4\text{Ph})_{18-x}(\text{SeC}_{12}\text{H}_{25})_x$  ( $x = 0-8$ ; entry 10), respectively. The chromatogram exhibits well defined peaks, indicating that the  $\text{Au}_{24}\text{Pd}(\text{SC}_2\text{H}_4\text{Ph})_{18-x}(\text{SeC}_{12}\text{H}_{25})_x$  ( $x = 0-8$ ) clusters were also separated with high resolution by this method. Although the extents of charge transfer in the Au-SeR and Au-SR ligands are different,<sup>32,34</sup> the retention times of the  $\text{Au}_{24}\text{Pd}(\text{SC}_2\text{H}_4\text{Ph})_{18-x}(\text{SeC}_{12}\text{H}_{25})_x$  ( $x = 0-8$ ) clusters are consistent with those of  $\text{Au}_{24}\text{Pd}(\text{SC}_2\text{H}_4\text{Ph})_{18-x}(\text{SC}_{12}\text{H}_{25})_x$  ( $x = 0-8$ ; Figure 2b). It was observed that  $\text{Au}_{24}\text{Pd}(\text{SC}_{12}\text{H}_{25})_{18-x}(\text{SeC}_{12}\text{H}_{25})_x$  (entry 11, Figure S11), in which both  $\text{SR}_1$  and  $\text{SeR}_2$  have  $\text{C}_{12}\text{H}_{25}$  as the functional group, did not undergo high-resolution separation by this method (Figure S13), suggesting that changes in the Au-ligand charge transfer have little effect on the polarity of the cluster surface. These results indicate that the  $\text{Au}_{24}\text{Pd}(\text{SC}_2\text{H}_4\text{Ph})_{18-x}(\text{SeC}_{12}\text{H}_{25})_x$  clusters underwent high-resolution separation as the result of the significant difference in the polarities of the SR and SeR functional groups. Thus, it should also be possible to isolate  $\text{Au}_{24}\text{Pd}(\text{SR}_1)_{18-x}(\text{SeR}_2)_x$  clusters when appropriate functional groups are applied. This leads us to expect that the extent of Au-ligand charge transfer<sup>32,34</sup> can be controlled by varying the relative proportions of  $\text{SR}_1$  and  $\text{SeR}_2$  ligands.

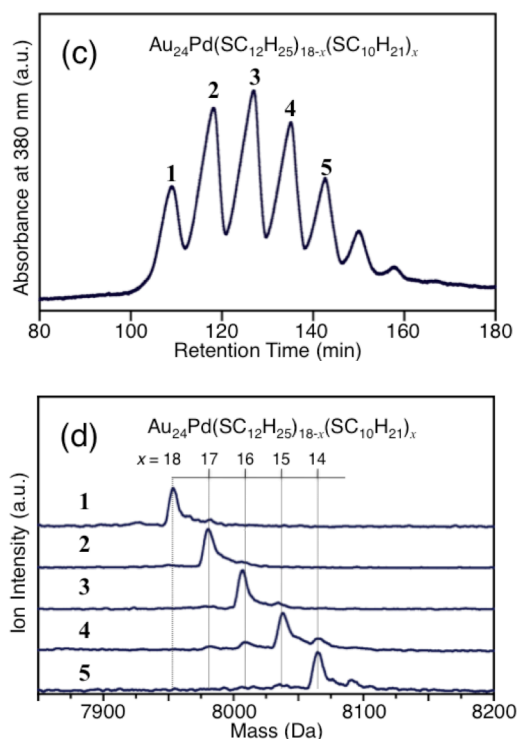


**Figure 3.** (a) Negative-ion MALDI mass spectrum, (b) chromatogram obtained with a linear gradient and (c) chromatogram obtained with a step gradient for  $\text{Au}_{24}\text{Pd}(\text{SC}_{12}\text{H}_{25})_{18-x}(\text{SC}_{10}\text{H}_{21})_x$  ( $x = 12-18$ ). When applying the linear gradient, no improvement in resolution was seen when increasing retention times by prolonging the mobile phase transition time.<sup>42</sup> (d) Negative-ion MALDI mass spectra of fractions 1-5 obtained by the fractionation of peaks 1-5 in (c).

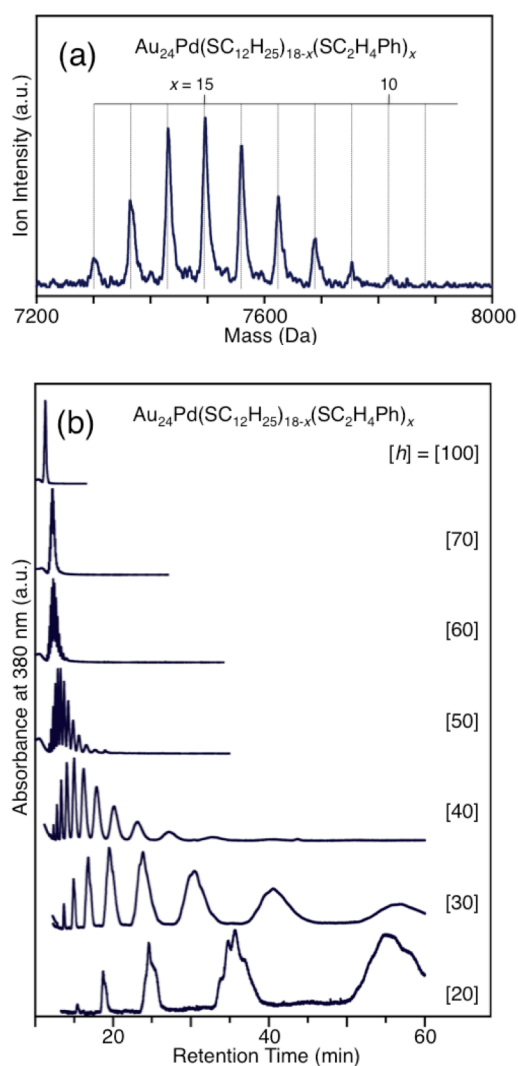


**Figure 4.** (a) Negative-ion MALDI mass spectrum and (b) chromatograms of  $\text{Au}_{24}\text{Pd}(\text{SC}_{12}\text{H}_{25})_{18-x}(\text{SC}_2\text{H}_4\text{Ph})_x$  ( $x = 10-18$ ) obtained with a step gradient, applying varying step heights  $[h]$  (see Chart 2). The mass spectrum in (a) is the same as that in Figure S6 (red line).

#### Gradient Program for Higher-Resolution Separation.

In the above experiments, a linear gradient was applied during the mobile phase substitution process (Chart 2).  $\text{Au}_{24}\text{Pd}(\text{SC}_{12}\text{H}_{25})_{18-x}(\text{SC}_{10}\text{H}_{21})_x$ , whose functional groups exhibit only a small polarity difference, cannot be separated with high resolution using this technique (Figure S14). However, we found that  $\text{Au}_{24}\text{Pd}(\text{SC}_{12}\text{H}_{25})_{18-x}(\text{SC}_{10}\text{H}_{21})_x$  can be isolated with high resolution when a step-gradient program is applied during the mobile phase substitution (Chart 2). As an example, the results obtained for  $\text{Au}_{24}\text{Pd}(\text{SC}_{12}\text{H}_{25})_{18-x}(\text{SC}_{10}\text{H}_{21})_x$  ( $x = 12-18$ ; Figure 3a) are shown in Figure 3. Figures 3b and 3c present chromatograms of this cluster series obtained using both a linear-gradient and a step-gradient mobile phase transition. The step height,  $[h]$ , associated with the step-gradient transition corresponds to the concentration of THF in the solvent (in volume %) following mobile phase substitution. A step height of [40] was applied in this experimental trial (Chart 2). As shown in Figure 3b, only a single, poorly-resolved peak is observed in the chromatogram

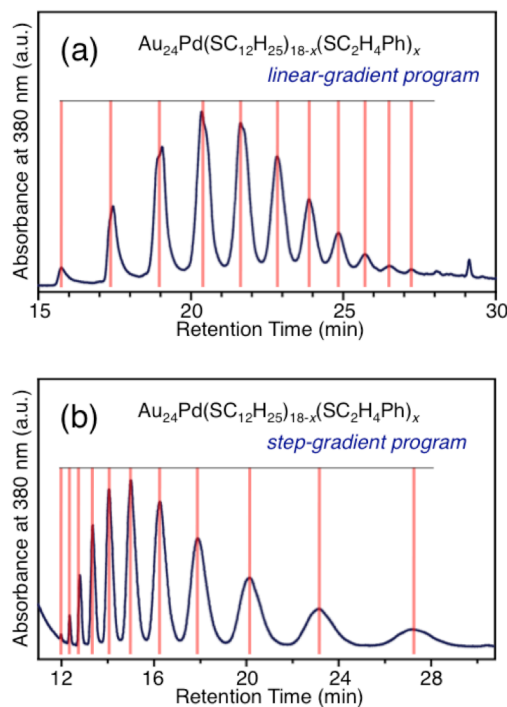


**Figure 5.** Comparison between chromatograms obtained with (a) a linear-gradient and (b) a step-gradient program ( $[h] = [40]$ ) for  $\text{Au}_{24}\text{Pd}(\text{SC}_{12}\text{H}_{25})_{18-x}(\text{SC}_2\text{H}_4\text{Ph})_x$  (Figure 4a).

obtained using the linear-gradient program. In contrast, when the step-gradient program was applied, clearly resolved peaks appeared in the resulting chromatogram (Figure 3c). Each peak was fractionated and the chemical compositions were determined using MALDI mass spectrometry (Figure 3d). The results revealed that each peak was composed solely of cluster with a single chemical composition, meaning that the  $\text{Au}_{24}\text{Pd}(\text{SC}_{12}\text{H}_{25})_{18-x}(\text{SC}_{10}\text{H}_{21})_x$  clusters were isolated with high resolution. It was also evident that, even when using this program, the clusters containing numerous high-polarity ligands were eluted into the mobile phase first, similar to the results obtained when applying the linear gradient (Figure 1). These results demonstrate that improved resolution of the clusters can be obtained when applying a step gradient during chromatography, as compared to the resolution achieved when a linear-gradient program is used.

It was found that the separation resolution achievable with this method varied greatly depending on the step height applied. Figure 4a shows the MALDI mass spectrum of  $\text{Au}_{24}\text{Pd}(\text{SC}_{12}\text{H}_{25})_{18-x}(\text{SC}_2\text{H}_4\text{Ph})_x$  ( $x = 10-18$ ) and Figure 4b shows the chromatograms obtained with different step heights. As the step height was reduced, the retention time increased, and accordingly, the interval between the individual peaks also increased. When the step height was lowered to [20], the peak separation became extremely clear, and moreover, a multiple peak structure was observed within each individual peak (Figure 4b). This type of peak structure has also been observed when a linear-gradient program was used (red line in entry 6, Figure 1).<sup>42</sup> However, the structures of these peaks were much clearer when the step-gradient program was used. It has been confirmed that rearrangement of ligands does not occur in this time scale<sup>42</sup> and thus these multiple sub-peaks are assumed to arise from coordination isomers<sup>42,43,52</sup>. These results imply that

a step-gradient program could be used to isolate even these isomers with relatively high resolution.

The significant difference in resolution between the linear and step gradients is considered to be related to the different separation mechanisms involved. When a linear gradient is applied during the mobile phase transition, the adsorbates (the clusters) are sequentially eluted into the mobile phase in order of surface polarity in response to the continuous transformation of the mobile phase (Chart 2). The strength of adsorption to the stationary phase is considered to control the retention time of each adsorbate, as in adsorption chromatography. However, when a step-gradient program is used for the substitution, the mobile phase is immediately transformed into a solvent that dissolves the adsorbate (Chart 2). In this case, the partition coefficient likely controls the retention time of each cluster, as in partition chromatography. Actually, the chromatograms obtained by each technique are significantly different; in the former case, the intervals between peaks in the chromatograms decrease with increasing retention times (Figure 5a), whereas in the latter case peak separations increase with increasing retention times (Figure 5b), supporting our interpretation that different separation mechanisms are involved in each case. This difference between the separation mechanisms (Figure S15) is considered to be strongly associated with the differences in resolution obtainable with the two techniques. The details of the different separation mechanisms connected with each mobile phase transition are expected to be elucidated by future experimental and theoretical studies.

**Advantages as an Analytical Method.** Finally, we describe the advantages of this technique as an analytical method. As noted, the ligand-exchange reaction allows the introduction of different ligands into the metal cluster. The quantity of exchanged ligands and their distribution are typically evaluated using mass spectrometry.<sup>25,26,51</sup> However, in situations where two types of ligands have comparable molecular weights, analysis of the ligand distribution using mass spectrometry is difficult. In contrast, our technique allows the separation of the metal clusters based on differences in the ligand polarities rather than their molecular weights. For this reason, if the polarities of two ligands differ, the ligand distributions of the cluster can be analyzed. As an example, Figure 6 shows the results obtained for  $\text{Au}_{24}\text{Pd}(\text{SC}_{12}\text{H}_{25})_{18-x}(\text{SCH}_2\text{PhBr})_x$  clusters, which are protected by  $\text{SC}_{12}\text{H}_{25}$  ( $M_{w_{av}} = 201.39$ ) and  $\text{SCH}_2\text{PhBr}$  ( $M_{w_{av}} = 202.09$ ); these two ligands have similar molecular weights (entry 5, Table 1). Only broad peaks were observed in the MALDI mass spectra of  $\text{Au}_{24}\text{Pd}(\text{SC}_{12}\text{H}_{25})_{18-x}(\text{SCH}_2\text{PhBr})_x$  obtained under any of the experimental reaction conditions (Figures 6a and S5) and assessment of the ligand distribution from such spectra is difficult. Considering that each individual  $\text{Au}_{24}\text{Pd}(\text{SC}_{12}\text{H}_{25})_{18-x}(\text{SCH}_2\text{PhBr})_x$  cluster has its own distribution of isotopes, analysis of the ligand distribution from the mass spectra remains challenging even when the measurements are performed using an ultrahigh-resolution mass spectrometer<sup>33,51</sup> rather than the mass spectrometer employed in this work (Figure S16). However, a clear peak separation was observed in the chromatograms of these  $\text{Au}_{24}\text{Pd}(\text{SC}_{12}\text{H}_{25})_{18-x}(\text{SCH}_2\text{PhBr})_x$  clusters (Figure 6b). The number of peaks observed is 19, and this number agrees with the number of possible ligand combinations for  $\text{Au}_{24}\text{Pd}(\text{SC}_{12}\text{H}_{25})_{18-x}(\text{SCH}_2\text{PhBr})_x$  ( $x = 0-18$ ). In the chromatogram, the rightmost peak can be attributed to  $\text{Au}_{24}\text{Pd}(\text{SC}_{12}\text{H}_{25})_{18}$  (Figure 1). Because  $\text{SCH}_2\text{PhBr}$  possesses a functional group that is more polar than  $\text{SC}_{12}\text{H}_{25}$ , the result can

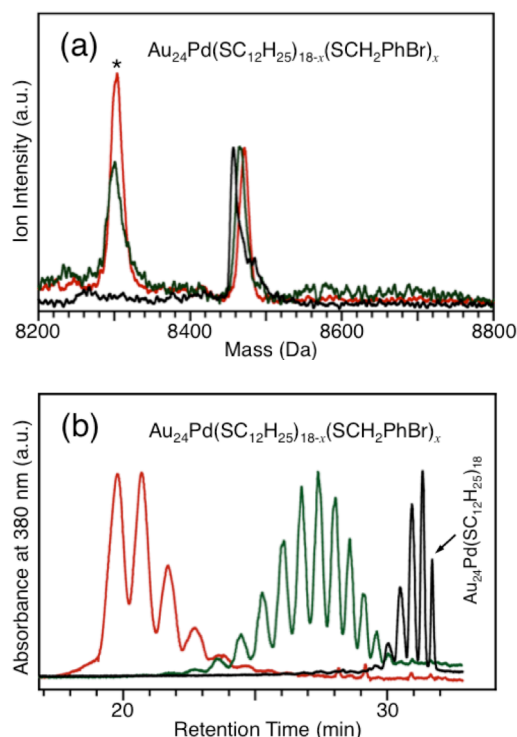


**Figure 6.** Comparison between (a) negative-ion MALDI mass spectra and (b) chromatograms obtained using a linear gradient for  $\text{Au}_{24}\text{Pd}(\text{SC}_{12}\text{H}_{25})_{18-x}(\text{SCH}_2\text{PhBr})_x$ . Between (a) and (b), the same color indicates the same sample and the colors refer to the ligand exchange reaction times: short (black), medium (green) and long (red). Thus  $x$  is small in the case of the black line, and progressively larger in the cases of the green and red lines. In (a), the asterisk indicates laser-induced fragments [ $\text{Au}_{24}\text{Pd}(\text{SC}_{12}\text{H}_{25})_{18-x}(\text{SCH}_2\text{PhBr})_{x-1}\text{S}$ ]. The chromatograms in (b) are the same as those in entry 5 of Figure 1. In (b), the rightmost peak is assigned to  $\text{Au}_{24}\text{Pd}(\text{SC}_{12}\text{H}_{25})_{18}$  (Figure 1).

be interpreted as the retention time of the  $\text{Au}_{24}\text{Pd}(\text{SC}_{12}\text{H}_{25})_{18-x}(\text{SCH}_2\text{PhBr})_x$  ( $x = 0-18$ ) decreasing as the number of  $\text{SCH}_2\text{PhBr}$  ligands increases. The ligand distribution can be readily estimated from such clearly separated chromatograms. Our method therefore has significant potential in terms of the analysis of the chemical compositions of metal clusters that are protected by two types of ligands with approximately equivalent molecular weights.

## Conclusions

This study revealed the suitable conditions and advanced use of a separation method involving a combination of reverse-phase HPLC and mobile-phase substitution with applications to the separation of  $\text{Au}_{24}\text{Pd}(\text{SR}_1)_{18-x}(\text{SR}_2)_x$  and  $\text{Au}_{24}\text{Pd}(\text{SR}_1)_{18-x}(\text{SeR}_2)_x$  clusters. The results obtained in this work are summarized as follows.

- (1) To ensure high-resolution separation of clusters, it is very important to increase the difference between the polarities of the functional groups on the two types of ligands. Suitable ligand combinations for separation can be predicted from the retention times of the  $\text{Au}_{24}\text{Pd}(\text{SR}_1)_{18}$  and  $\text{Au}_{24}\text{Pd}(\text{SR}_2)_{18}$ , which cause the terminal peaks of a series of peaks.
- (2)  $\text{Au}_{24}\text{Pd}(\text{SR}_1)_{18-x}(\text{SR}_2)_x$  can be isolated with improved resolution using a step-gradient mobile phase transition,

compared to the results obtained when applying a linear gradient.

(3) The reported method also has significant potential for use in the analysis of the chemical compositions of metal clusters protected by two types of ligands with approximately equivalent molecular weights.

Our previous work demonstrated that this method is also applicable to  $\text{Au}_{25}(\text{SR}_1)_{18-x}(\text{SR}_2)_x$  and  $\text{Au}_{38}(\text{SR}_1)_{24-x}(\text{SR}_2)_x$  clusters which have metal cores other than  $\text{Au}_{24}\text{Pd}^{42}$  and the above conclusions are also expected to hold true for these clusters. We believe that the results of this study serve to improve our understanding of the high-resolution isolation of metal clusters and will be helpful in future work related to designing specific metal clusters via control of the ligand composition.

## Experiments

**Synthesis of mixtures of  $\text{Au}_{24}\text{Pd}$  clusters with two different types of ligands.**  $\text{Au}_{24}\text{Pd}(\text{SR}_1)_{18-x}(\text{SR}_2)_x$  and  $\text{Au}_{24}\text{Pd}(\text{SR}_1)_{18-x}(\text{SeR}_2)_x$  were synthesized by the ligand-exchange reaction between  $\text{Au}_{24}\text{Pd}(\text{SR}_1)_{18}$  and  $\text{R}_2\text{SH}$  or  $(\text{R}_2\text{Se})_2$ .<sup>42,51</sup> First,  $\text{Au}_{24}\text{Pd}(\text{SC}_{12}\text{H}_{25})_{18}$  and  $\text{Au}_{24}\text{Pd}(\text{SC}_2\text{H}_4\text{Ph})_{18}$  were synthesized using a previously reported method,<sup>45</sup> or with slight modifications. Then,  $\text{Au}_{24}\text{Pd}(\text{SC}_{12}\text{H}_{25})_{18}$  (0.1  $\mu\text{mol}$ ) or  $\text{Au}_{24}\text{Pd}(\text{SC}_2\text{H}_4\text{Ph})_{18}$  (0.1  $\mu\text{mol}$ ) was dissolved in 1 mL of dichloromethane and  $\text{R}_2\text{SH}$  (10–100  $\mu\text{mol}$ ) or  $(\text{R}_2\text{Se})_2$  (10–100  $\mu\text{mol}$ ) was added with stirring at room temperature, after which the reaction was allowed to progress for the desired length of time. The solution was then evaporated to dryness and washed with a mixture of methanol and water to remove excess thiols or diselenides, and the product was characterized by matrix-assisted laser desorption–ionization (MALDI) mass spectrometry (Figures S1–S11).  $\text{Au}_{24}\text{Pd}(\text{SR}_1)_{18-x}(\text{SR}_2)_x$  clusters with various chemical compositions were synthesized by changing the quantity of thiol ( $\text{R}_2\text{SH}$ ) added to the reaction mixture as well as varying the reaction time (Figures S1–S9).

**HPLC analyses.** A Shimadzu Prominence HPLC (Chart S2) was used to separate the clusters into unique ligand combination. A Thermo Scientific Hypersil C18 column (250 mm  $\times$  4.6 mm i.d.) (Figure S17 and Table S1) was used as the reverse phase column and was held at 25  $^\circ\text{C}$  to ensure reproducibility (Figure S18 and Table S2). In the experiments, first, methanol (Figure S19 and Table S3), in which the  $\text{Au}_{24}\text{Pd}$  clusters are insoluble, was used as the mobile phase, and a suspension of the clusters was injected into the column; the clusters were all adsorbed onto the stationary phase. Next, the mobile phase was continuously substituted by a solvent that dissolves the clusters (tetrahydrofuran (THF); Figure S20 and Table S4), and the clusters were sequentially eluted into the mobile phase.

**MALDI mass spectrometry.** MALDI mass spectra were acquired with a time-of-flight mass spectrometer (JEOL Ltd., JMS-S3000) using an Nd:YAG laser (wavelength: 349 nm) and DCTB as the MALDI matrix. The cluster-to-matrix ratio was set at 1:1000 and the laser fluence was reduced to the lowest value that enabled ions to be detected. All the spectra were obtained in negative-ion mode.

## Acknowledgements

We thank Tatsuya Ohyama, Tafu Nakazaki, Keita Kanehira, Masaki Yamaguchi and Makoto Eguro for providing technical assistance and Wataru Kurashige for his valuable comments. This work was financially supported by research grants from the Saito Houonkai Foundation and TEPCO Memorial foundation as well as a Grant-in-Aid for Scientific Research (No. 25288009 and 25102539) from the Ministry of Education, Culture, Sports, Science and Technology (MEXT) of Japan.

## Notes and references

<sup>a</sup> Department of Applied Chemistry, Faculty of Science, Tokyo University of Science, 1-3 Kagurazaka, Shinjuku-ku, Tokyo 162-8601, Japan.

<sup>b</sup> Photocatalysis International Research Center, Tokyo University of Science, 2641 Yamazaki, Noda, Chiba 278-8510, Japan.

† Electronic Supplementary Information (ESI) available: Details of chemical reagents and products, analysis and product characterization. See DOI: 10.1039/b000000x/

- 1 M. Brust, M. Walker, D. Bethell, D. J. Schiffrin and R. Whyman, *J. Chem. Soc., Chem. Commun.*, 1994, 801–802.
- 2 R. L. Whetten, M. N. Shafiqullin, J. T. Khoury, T. G. Schaaff, I. Vezmar, M. M. Alvarez and A. Wilkinson, *Acc. Chem. Res.*, 1999, **32**, 397–406.
- 3 J. F. Parker, C. A. Fields-Zinna and R. W. Murray, *Acc. Chem. Res.*, 2010, **43**, 1289–1296.
- 4 T. Tsukuda, *Bull. Chem. Soc. Jpn.*, 2012, **85**, 151–168.
- 5 H. Häkkinen, *Nat. Chem.*, 2012, **4**, 443–455.
- 6 T. Udayabhaskararao and T. Pradeep, *J. Phys. Chem. Lett.*, 2013, **4**, 1553–1564.
- 7 H. Qian, M. Zhu, Z. Wu and R. Jin, *Acc. Chem. Res.*, 2012, **45**, 1470–1479.
- 8 A. C. Dharmaratne, T. Krick and A. Dass, *J. Am. Chem. Soc.*, 2009, **131**, 13604–13605.
- 9 Y. Yu, Q. Yao, Z. Luo, X. Yuan, J. Y. Lee and J. Xie, *Nanoscale*, 2013, **5**, 4606–4620.
- 10 C. M. Aikens, *J. Phys. Chem. Lett.*, 2011, **2**, 99–104.
- 11 D.-e. Jiang, *Nanoscale*, 2013, **5**, 7149–7160.
- 12 M. Walter, J. Akola, O. Lopez-Acevedo, P. D. Jadzinsky, G. Calero, C. J. Ackerson, R. L. Whetten, H. Grönbeck and H. Häkkinen, *Proc. Natl. Acad. Sci. U.S.A.*, 2008, **105**, 9157–9162.
- 13 Y. Negishi, W. Kurashige, Y. Niihori and K. Nobusada, *Phys. Chem. Chem. Phys.*, 2013, **15**, 18736–18751.
- 14 T. P. Bigioni and R. L. Whetten, *Ö. Dag, J. Phys. Chem. B*, 2000, **104**, 6983–6986.
- 15 G. Li and R. Jin, *Acc. Chem. Res.*, 2013, **46**, 1749–1758.
- 16 Y. Li, O. Zaluzhna, B. Xu, Y. Gao, J. M. Modest and Y. Y. J. Tong, *J. Am. Chem. Soc.*, 2011, **133**, 2092–2095.
- 17 T. G. Schaaff and R. L. Whetten, *J. Phys. Chem. B*, 2000, **104**, 2630–2641.
- 18 Y. Negishi, K. Nobusada and T. Tsukuda, *J. Am. Chem. Soc.*, 2005, **127**, 5261–5270.
- 19 M. M. F. Choi, A. D. Douglas and R. W. Murray, *Anal. Chem.*, 2006, **78**, 2779–2785.
- 20 X. Yang, Y. Su, M. C. Paau and M. M. F. Choi, *Anal. Chem.*, 2012, **84**, 1765–1771.

- 21 R. L. Whetten, J. T. Khoury, M. M. Alvarez, S. Murthy, I. Vezmar, Z. L. Wang, P. W. Stephens, C. L. Cleveland, W. D. Luedtke and U. Landman, *Adv. Mater.*, 1996, **8**, 428–433.
- 22 Y. Negishi, N. K. Chaki, Y. Shichibu, R. L. Whetten and T. Tsukuda, *J. Am. Chem. Soc.*, 2007, **129**, 11322–11323.
- 23 R. L. Wolfe and R. W. Murray, *Anal. Chem.*, 2006, **78**, 1167–1173.
- 24 Y. Negishi, C. Sakamoto, T. Ohyama and T. Tsukuda, *J. Phys. Chem. Lett.*, 2012, **3**, 1624–1628.
- 25 J. B. Tracy, G. Kalyuzhny, M. C. Crowe, R. Balasubramanian, J.-P. Choi and R. W. Murray, *J. Am. Chem. Soc.*, 2007, **129**, 6706–6707.
- 26 A. Dass, A. Stevenson, G. R. Dubay, J. B. Tracy and R. W. Murray, *J. Am. Chem. Soc.*, 2008, **130**, 5940–5946.
- 27 C. A. Fields-Zinna, J. S. Sampson, M. C. Crowe, J. B. Tracy, J. F. Parker, A. M. deNey, D. C. Muddiman and R. W. Murray, *J. Am. Chem. Soc.*, 2009, **131**, 13844–13851.
- 28 H. Qian, Y. Zhu and R. Jin, *Proc. Natl. Acad. Sci. U.S.A.*, 2012, **109**, 696–700.
- 29 Z. Wu and R. Jin, *Nano Lett.*, 2010, **10**, 2568–2573.
- 30 Y. Kim, R. C. Johnson and J. T. Hupp, *Nano Lett.*, 2001, **1**, 165–167.
- 31 M. Brust, N. Stuhr-Hansen, K. Nørgaard, J. B. Christensen, L. K. Nielsen and T. Bjørnholm, *Nano Lett.*, 2001, **1**, 189–191.
- 32 Y. Negishi, W. Kurashige, U. Kamimura, *Langmuir*, 2011, **27**, 12289–12292.
- 33 W. Kurashige, M. Yamaguchi, K. Nobusada and Y. Negishi, *J. Phys. Chem. Lett.*, 2012, **3**, 2649–2652.
- 34 W. Kurashige, S. Yamazoe, K. Kanehira, T. Tsukuda and Y. Negishi, *J. Phys. Chem. Lett.*, 2013, **4**, 3181–3185.
- 35 X. Meng, Q. Xu, S. Wang and M. Zhu, *Nanoscale* 2012, **4**, 4161–4165.
- 36 Z. Tang, D. A. Robinson, N. Bokossa, B. Xu, S. Wang and G. Wang, *J. Am. Chem. Soc.*, 2011, **133**, 16037–16044.
- 37 D. Zanchet, C. M. Micheel, W. J. Parak, D. Gerion and A. P. Alivisatos, *Nano Lett.*, 2001, **1**, 32–35.
- 38 C. J. Ackerson, P. D. Jadzinsky, G. J. Jensen and R. D. Kornberg, *J. Am. Chem. Soc.*, 2006, **128**, 2635–2640.
- 39 J. G. Worden, Q. Dai, A. W. Shaffer and Q. Huo, *Chem. Mater.*, 2004, **16**, 3746–3755.
- 40 S. Park and K. Hamad-Schifferli, *J. Phys. Chem. C*, 2008, **112**, 7611–7616.
- 41 S. Knoppe, R. Azoulay, A. Dass and T. Bürgi, *J. Am. Chem. Soc.*, 2012, **134**, 20302–20305.
- 42 Y. Niihori, M. Matsuzaki, T. Pradeep and Y. Negishi, *J. Am. Chem. Soc.*, 2013, **135**, 4946–4949.
- 43 L. Beqa, D. Deschamps, S. Perrio, A.-C. Gaumont, S. Knoppe and T. Bürgi, *J. Phys. Chem. C*, 2013, **117**, 21619–21625.
- 44 C. A. Fields-Zinna, M. C. Crowe, A. Dass, J. E. F. Weaver and R. W. Murray, *Langmuir*, 2009, **25**, 7704–7710.
- 45 Y. Negishi, W. Kurashige, Y. Niihori, T. Iwasa and K. Nobusada, *Phys. Chem. Chem. Phys.*, 2010, **12**, 6219–6225.
- 46 Y. Negishi, W. Kurashige, Y. Kobayashi, S. Yamazoe, N. Kojima, M. Seto and T. Tsukuda, *J. Phys. Chem. Lett.*, 2013, **4**, 3579–3583.
- 47 R. Guo, Y. Song, G. Wang and R. W. Murray, *J. Am. Chem. Soc.*, 2005, **127**, 2752–2757.
- 48 V. R. Jupally, R. Kota, E. V. Dornshuld, D. L. Mattern, G. S. Tschumper, D.-e. Jiang and A. Dass, *J. Am. Chem. Soc.*, 2011, **133**, 20258–20266.
- 49 M. S. Devadas, K. Kwak, J.-W. Park, J.-H. Choi, C.-H. Jun, E. Sinn, G. Ramakrishna and D. Lee, *J. Phys. Chem. Lett.*, 2010, **1**, 1497–1503.
- 50 C. L. Heinecke, T. W. Ni, S. Malola, V. Mäkinen, O. A. Wong, H. Häkkinen and C. J. Ackerson, *J. Am. Chem. Soc.*, 2012, **134**, 13316–13322.
- 51 Y. Niihori, W. Kurashige, M. Matsuzaki and Y. Negishi, *Nanoscale*, 2013, **5**, 508–512.
- 52 J. F. Parker, K. A. Kacprzak, O. Lopez-Acevedo, H. Häkkinen and R. W. Murray, *J. Phys. Chem. C*, 2010, **114**, 8276–8281.